J|A|C|S
ARTICLES

Published on Web 03/26/2010

Synthesis, Structure, Spirocyclization Mechanism, and Glutathione Peroxidase-like Antioxidant Activity of Stable Spirodiazaselenurane and Spirodiazatellurane

Bani Kanta Sarma,[†] Debasish Manna,[†] Mao Minoura,[‡] and Govindasamy Mugesh*[,†]

Department of Inorganic and Physical Chemistry, Indian Institute of Science, Bangalore 560 012, India, and Department of Chemistry, School of Science, Kitasato University, Kanagawa, 228-8555, Japan

Received September 22, 2009; E-mail: mugesh@ipc.iisc.ernet.in

Abstract: The first examples of stable spirodiazaselenurane and spirodiazatellurane were synthesized by oxidative spirocyclization of the corresponding diaryl selenide and telluride and were structurally characterized. X-ray crystal structures of the spirodiazaselenurane and spirodiazatellurane suggest that the structures are distorted trigonal bipyramidal (TBP) with the electronegative nitrogen atoms occupying the apical positions and two carbon atoms and the lone pair of Se/Te occupying the equatorial positions. Interestingly, the spirodiazatellurane underwent spontaneous chiral resolution during crystallization, and the absolute configurations of its enantiomers were confirmed by single-crystal X-ray analyses. A detailed mechanistic study indicates that the cyclization to spirodiazaselenurane and spirodiazatellurane occurs via selenoxide and telluroxide intermediates. The chalcogenoxides cyclize to the corresponding spiro compounds in a stepwise manner via the involvement of hydroxyl chalcogenurane intermediates, and the activation energy for the spirocyclization reaction decreases in the order S > Se > Te. In addition to the synthesis, characterization, and mechanism of cyclization, the glutathione peroxidase (GPx) mimetic activity of the newly synthesized compounds was evaluated. These studies suggest that the tellurium compounds are more effective as GPx mimics than their selenium counterparts due to the fast oxidation of the tellurium center in the presence of peroxide and the involvement of an efficient redox cycle between the telluride and telluroxide intermediate.

Introduction

The chemistry of spirodioxysulfuranes has been studied extensively due to their interesting structural and stereochemical properties.[1] In addition to the sulfur compounds, some selenium and tellurium analogues have also been studied.[2] The first compound of this kind, spirodioxyselenurane **2**, was synthesized in 1914 by Lesser and Weiss.[3] Subsequently the sulfur[1a] and tellurium[2a] analogues of **2**, compounds **1** and **3**, respectively, were also synthesized. Further, unsymmetrical spirochalcogenuranes such as **4**−**6**,[4−6] spirosulfuranes with rings of different sizes within the same molecule such as **7** and **8**,[7] and spirosulfuranes having different electronegative atoms in the apical positions such as **9** and **10**[8] have also been reported. Several of these spirochalcogenuranes were synthesized by reacting the parent chalcogenides with a halogenating agent such as chloramines-T, chlorine, or bromine.[9] Another method for the synthesis of spirodioxysulfuranes was suggested by Martin and co-workers, which involved the treatment of the parent sulfide with KH followed by bromination.[10,11] However, the

[†] Indian Institute of Science.
[‡] Kitasato University.

(1) (a) Kapovits, I.; Kálmán, A. *Chem. Commun.* **1971**, 649–650. (b) Martin, J. C.; Perozzi, E. F. *Science* **1976**, *191*, 154–159. (c) Martin, J. C. *Science* **1983**, *221*, 509–514. (d) Hayes, R. A.; Martin, J. C. In *Sulfurane Chemistry*; Bernardi, F., Csizmadia, I. G., Mangini, A., Eds.; Elsevier: Amsterdam, 1985; pp 408−483. (e) Drabowicz, J.; Lyzwa, P.; Mikolajczyk, M. In *High-Coordinated Sulfur Compounds*; Patai, S., Rappoport, Z., Eds.; Wiley: New York, 1993; pp 799−956. (f) Drabowicz, J.; Martin, J. C. *Pure Appl. Chem.* **1996**, *68*, 951–956. (g) Drabowicz, J. In *Hypervalent Sulfuranes As Transient and Isolable Structures: Occurrence, Synthesis and Reactivity*; Akiba, K.-Y., Ed.; Wiley: New York, 1999; pp 211−240. (h) Furukawa, N.; Sato, S. *Top. Curr. Chem.* **1999**, *205*, 89–129.

(2) (a) Takaguchi, Y.; Furukawa, N. *Heteroat. Chem.* **1995**, *6*, 481–484. (b) Furukawa, N.; Sato, S. In *Structure and Reactivity of Hypervalent Chalcogen Compounds: Selenurane (Selane) and Tellurane (Tellane)*; Akiba, K.-Y., Eds.; Wiley: New York, 1999; pp 241−278. (c) Drabowicz, J.; Halaba, G. *Rev. Heteroat. Chem.* **2000**, *22*, 1–32. (d) Takaguchi, Y.; Furukawa, N. *Chem. Lett.* **1996**, *5*, 365–366. (e) Zhang, J.; Takahashi, S.; Saito, S.; Koizumi, T. *Tetrahedron: Asymmetry* **1998**, *9*, 3303–3317. (f) Ohno, F.; Kawashima, T.; Okazaki, R. *Chem. Commun.* **2001**, 463–464. (g) Kano, N.; Takahashi, T.; Kawashima, T. *Tetrahedron Lett.* **2002**, *43*, 6775–6778. (h) Ohno, F.; Kawashima, T.; Okazaki, R. *Chem. Commun.* **1997**, *17*, 1671–1672. (i) Allenmark, S. *Chirality* **2008**, *20*, 544–551, and references therein.

(3) Lesser, R.; Weiss, R. *V. Ber. Dtsch. Chem. Ges.* **1914**, *47*, 2510–2525.

(4) Zhang, J.; Saito, S.; Koizumi, T. *J. Org. Chem.* **1998**, *63*, 9375–9384.

(5) Zhang, J.; Saito, S.; Koizumi, T. *J. Am. Chem. Soc.* **1998**, *120*, 1631–1632.

(6) Zhang, J.; Takahashi, S.; Saito, S.; Koizumi, T. *Tetrahedron: Asymmetry* **1998**, *9*, 3303–3317.

(7) Kapovits, I.; Rábai, J.; Szabó, D.; Czakó, K.; Kucsman, Á.; Argay, G.; Fülöp, V.; Kálmán, A.; Koritsánsky, T.; Párkányi, L. *J. Chem. Soc., Perkin Trans. 2* **1993**, 847–853.

(8) Szókán, G.; Szarvas, S.; Majer, Z.; Szabó, D.; Kapovits, I.; Hollósi, M. *J. Liq. Chromatogr.* **1999**, *22*, 993–1007.

(9) Kapovits, I.; Rábai, J.; Ruff, F.; Kucsman, Á. *Tetrahedron* **1979**, *35*, 1869–1874.

(10) Martin, J. C.; Perozzi, E. F. *J. Am. Chem. Soc.* **1974**, *96*, 3155–3168.

 10.1021/ja908080u

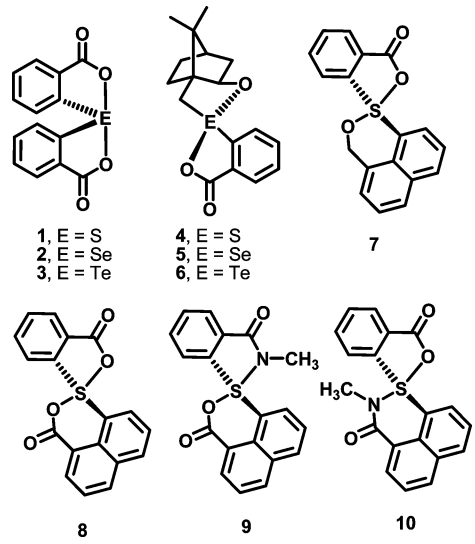

Figure 1. Examples of some spirochalcogenuranes with symmetric and asymmetric rings.

most convenient method to prepare spirochalcogenide involves cyclodehydration of the corresponding chalcogenoxides [E-oxide (E═O); E = S, Se, Te] obtained by treating the parent chalcogenides with oxidizing agents such as H_2O_2.[12] While the selenoxides and telluroxides can undergo spontaneous cyclization, the conversion of sulfoxides to the corresponding spirosulfuranes requires a dehydrating agent.[2i] The pioneering work on spirosulfuranes by Martin and co-workers[10,13] and Kapovits and co-workers[1a,7,14] clearly demonstrated the significantly increased chemical stability of the spirocyclic systems compared to their open-chain analogues. Furthermore, it has been observed that the reactivity of spirocyclic systems is determined by the size of the largest spiro-ring, which is easily opened but does not take a significant part in any ring-closure equilibrium.[14b] It was also suggested that the stability of the spirochalcogenuranes toward hydrolysis increases with the increase in the size of the central atom; thus, for spirodioxychalcogenuranes **1**−**3** the stability toward hydrolysis follows the order **1** < **2** < **3**.[2i]

Recently, Back and co-workers[15] have shown that the spirodioxyselenurane **11** and its homologues act as efficient mimics of glutathione peroxidase (GPx), a selenoenzyme that protects various organisms from oxidative damage by catalyzing the reduction of harmful peroxides in the presence of glutathione (GSH).[16] The tellurium analogue **12** displayed much higher activity than **11**, whereas the aromatic derivatives **2** and **13** exhibited much lower catalytic activity as compared to that of

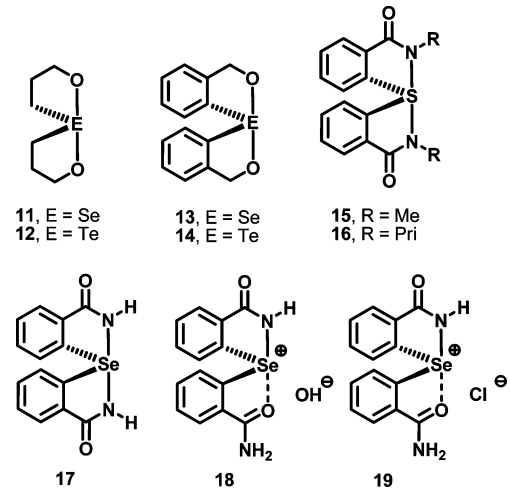

Figure 2. Examples of some chalcogenurane and related compounds.

the aliphatic compounds.[17] In contrast to spirodioxysulfuranes, which have two oxygen atoms in the apical positions, the spirodiazasulfuranes, having two nitrogen atoms, are extremely rare. While the nitrogen-substituted spirodiazasulfurane **16** and some related compounds have been investigated,[18] there is no structural evidence for stable spirodiazaselenuranes or spirodiazatelluranes. Very recently, Back and co-workers have demonstrated the relative instability of spirodiazaselenuranes.[19] They have shown that the reaction of 2,2′-selenobis(benzamide) with H_2O_2 or *N*-chlorosuccinimide (NCS) does not afford the expected spirodiaza derivative **17**, but it produces the corresponding azaselenonium hydroxide (**18**) and azaselenonium chloride (**19**), respectively. Further, on the basis of the ^{1}H NMR spectrum, it was suggested that the azaselenonium chloride **19** upon reaction with an excess of KH produces a hydrolytically unstable spirodiazaselenurane as a dipotassium salt.[19]

In this paper, we report that the reactions of 2,2′-selenobis(benzanilide) (**20**) and 2,2′-tellurobis(benzanilide) (**21**) with H_2O_2/t-BuOOH afford the first examples of stable spirodiazaselenurane (**24**) and spirodiazatellurane (**25**), respectively (Scheme 1). These observations indicate that the substituents attached to the amide nitrogen atoms may play an important role in the stability of spirodiazachalcogenuranes. Further, we report a detailed theoretical mechanistic investigation on the cyclization of E-oxide (E = S, Se, Te) to the corresponding spirodiazachalcogenurane. The theoretical studies suggest that the spirocyclization of E-oxide occurs via a trigonal-bipyramidal intermediate (TBP) and the telluroxides cyclize much faster than their sulfur and selenium analogues. We also demonstrate that

(11) Adzima, L. J.; Martin, J. C. *J. Org. Chem.* **1977**, *42*, 4006–4016.
(12) Kapovits, I.; Rabai, J.; Ruff, F.; Kucsman, Á.; Tanács, B. *Tetrahedron* **1979**, *35*, 1875–1881.
(13) (a) Martin, J. C.; Arhart, R. J. *J. Am. Chem. Soc.* **1971**, *93*, 2339–2341. (b) Martin, J. C.; Arhart, R. J. *J. Am. Chem. Soc.* **1971**, *93*, 2341–2342. (c) Arhart, R. J.; Martin, J. C. *J. Am. Chem. Soc.* **1972**, *94*, 4997–5003. (d) Perozzi, E. F.; Martin, J. C. *J. Am. Chem. Soc.* **1972**, *94*, 5519–5520.
(14) (a) Kálmán, A.; Sasvári, K.; Kapovits, I. *Acta Crystallogr. Sect. B* **1973**, *29*, 355–357. (b) Vass, E.; Ruff, F.; Kapovits, I.; Rábai, J.; Szabó, D. *J. Chem. Soc., Perkin Trans. 2* **1993**, 855–859.
(15) Back, T. G.; Moussa, Z.; Parvez, M. *Angew. Chem., Int. Ed.* **2004**, *43*, 1268–1270.
(16) (a) Flohé, L.; Günzler, E. A.; Schock, H. H. *FEBS Lett.* **1973**, *32*, 132–134. (b) Rotruck, J. T.; Pope, A. L.; Ganther, H. E.; Swanson, A. B.; Hafeman, D. G.; Hoekstra, W. G. *Science* **1973**, *179*, 588–590. (c) Epp, O.; Ladenstein, R.; Wendel, A. *Eur. J. Biochem.* **1983**, *133*, 51–69. (d) Jacob, C.; Giles, G. I.; Giles, N. M.; Sies, H. *Angew. Chem., Int. Ed.* **2003**, *42*, 4742–4758.
(17) (a) Back, T. G.; Kuzma, D.; Parvez, M. *J. Org. Chem.* **2005**, *70*, 9230–9236. (b) Tripathi, S. K.; Patel, U.; Roy, D.; Sunoj, R. B.; Singh, H. B.; Wolmershäuser, G.; Butcher, R. J. *J. Org. Chem.* **2005**, *70*, 9237–9247.
(18) (a) Adzima, L. J.; Martin, J. C. *J. Org. Chem.* **1977**, *42*, 4006–4016. (b) Adzima, L. J.; Chiang, C. C.; Paul, I. C.; Martin, J. C. *J. Am. Chem. Soc.* **1978**, *100*, 953–962. (c) Szabó, D.; Adám, T.; Kapovits, I. *Sulfur Lett.* **1997**, *21*, 21–34. (d) Szabó, D.; Kuti, M.; Kapovits, I.; Rábai, J.; Kucsman, A.; Argay, G.; Czugler, M.; Kálmán, A.; Párkányi, L. *J. Mol. Struct.* **1997**, *415*, 1–16. (e) Adám, T.; Ruff, F.; Kapovits, I.; Szabó, D.; Kucsman, A. *J. Chem. Soc., Perkin Trans. 2* **1998**, 1269–1275.
(19) Kuzma, D.; Parvez, M.; Back, T. G. *Org. Biomol. Chem.* **2007**, *5*, 3213–3217.

Scheme 1. Synthesis of Spirodiazaselenurane **24** and Its Tellurium Analogue **25**

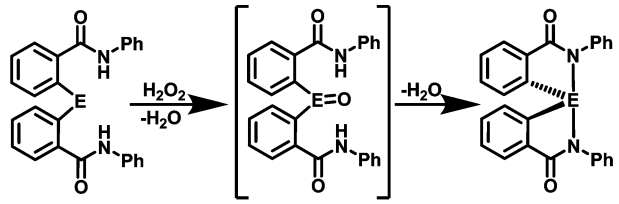

20, E = Se; **21**, E = Te **22**, E = Se; **23**, E = Te **24**, E = Se; **25**, E = Te

the monotelluride **21** exhibits high glutathione peroxidase (GPx) activity by catalyzing the reduction of t-BuOOH by benzyl thiol (BnSH).

Results and Discussion

Synthesis and Characterization of Spirodiazaselenurane and Spirodiazatellurane. The selenide **20** and telluride **21** were prepared by *ortho*-lithiation of benzanilide followed by $Se(dtc)_2$ or $Te(dtc)_2$ (dtc = diethyldithiacarbamate) addition and aqueous workup. The selenide **20** crystallized in the *C*2/*c* space group with half of the molecule in each asymmetric unit and four molecules in the unit cell. The geometry around the Se atom is V shaped with a C1−Se−C1 angle of 93.75(9)°. Owing to the presence of two O-donor atoms and the possibility of intramolecular nonbonded interaction[20] with the Se atom, it is possible that either one or both Se···O coordination bonds may be formed in **20**. The nonbonded Se···O distance (3.234 Å) is significantly higher than the sum of the single-bond covalent radii for selenium (1.17 Å) and oxygen (0.66 Å), but considerably shorter than their sum of van der Waals radii (3.42 Å). This distance is also higher than the Se···O bond distance observed in (phenylseleno)iminoquinone (2.476 Å)[21] and bis(*o*-formylphenyl) selenide[22] (2.806 Å). A look at the structure shows that the oxygen atoms form the characteristic envelope over the Se atom (O−Se−O = 159.6°), which would facilitate the formation of the five-membered rings (*cis*-conformation). This arrangement around the selenium atom is similar to that observed in bis[2-(dimethylaminomethyl)phenyl] selenide,[23] where two nitrogen atoms form the characteristic envelope over the Se atom. This arrangement is, however, quite different from the one observed in bis(*o*-formylphenyl) selenide,[22] in which one oxygen atom is involved in nonbonded interaction with the selenium atom and the other oxygen atom stays away, forming a linear O(1A)−Se−C(1B) geometry (∠O(1A)−Se−C(1B) = 166.5°).[22] Other bond length and angles in selenide **20** are in the normal range observed for related compounds.

The oxidation of **20** and **21** by H_2O_2/t-BuOOH afforded the spirodiazaselenurane **24** and spirodiazatellurane **25**, respectively, in nearly quantitative yield. It may be noted that the spirodiazatellurane can also be produced from the telluride **21** even in the absence of any oxidizing agent.[24] In contrast to the spirodiazasulfurane **16**, which was shown to be hydrolytically very labile,[18b] compounds **24** and **25** are found to be stable both in the solid state and in solution. The ^1H, ^{77}Se (for **24**) and ^{125}Te (for **25**) NMR spectra recorded in $CDCl_3$ in the presence of 50 μL of water did not show any hydrolysis of the spiro-rings (Figures S25−S28, Supporting Information). Single-crystal X-ray analyses indicate that the selenium and tellurium centers in compounds **24** and **25** adopt distorted trigonal bipyramidal (TBP) geometries with the electronegative nitrogen atoms (N1 and N2) occupying the apical positions and the two carbon atoms and lone pairs of Se/Te occupying the equatorial positions (Figure 3). The TBP geometry is more distorted in **25** than in **24** [∠N1(apical)−Te1−N2(apical): 162.91°; ∠N1(apical)−Se1−N2(apical): 174.29°]. Interestingly, the racemic spirodiazatellurane **25** underwent a spontaneous chiral resolution during the crystallization to afford the compound in two different enantiomeric forms. The X-ray data sets indicate that both the enantiomers crystallize in the chiral space group $P2_12_12_1$ of the orthorhombic system. Refinement of the Flack enantiopole parameter[25] led to a value of ~0, thus confirming the enantiomeric purity and absolute structure of the crystals. Although spirochalcogenuranes are expected to be chiral, to our knowledge, optically pure spirodiazachalcogenuranes have not yet been reported.[26] In contrast to the spontaneous resolution of tellurane **25**, no such phenomenon was observed in the case of **24**, which crystallized as a racemate ($P2_1/n$ space group).

Mechanism of Spirocyclization. The cyclization of the selenide and telluride to the corresponding spiro compounds was too fast at room temperature (25 °C) to detect the intermediates involved in the cyclization. It is observed that the selenide (**20**) reacted with H_2O_2 much slower than the telluride (**21**), and no oxidation of the selenium center in **20** was observed at −20 °C. Therefore, we were unable to detect the formation of the expected selenoxide **22** by NMR spectroscopy. When the telluride **21** was treated with H_2O_2 at −20 °C, a peak at 972 ppm was observed in ^{125}Te NMR spectroscopy, which can be assigned to the telluroxide **23** (Figure S29, Supporting Information). However, when the temperature was brought to 20 °C, the telluroxide (**23**) was converted completely to the spiro compound **25** (Figure S30, Supporting Information). As the selenide **20** is unreactive toward H_2O_2 at low temperatures, we synthesized compound **26**, in which the N−H moiety is replaced by an N−Me group. The replacement of N−H by a N−Me group would block the cyclization reaction, allowing isolation and characterization of the intermediate involved in the cyclization. As expected, the reaction of **26** with H_2O_2 produced the corresponding selenoxide **27**, which was purified and

(20) For excellent articles on Se···X (X = N, O, Cl, Br, F, etc.) interactions, see: (a) Iwaoka, M.; Tomoda, S. *Phosphorus, Sulfur Silicon Relat. Elem.* **1992**, *67*, 125–130. (b) Iwaoka, M.; Tomoda, S. *J. Am. Chem. Soc.* **1994**, *116*, 2557–2561. (c) Iwaoka, M.; Tomoda, S. *J. Am. Chem. Soc.* **1996**, *118*, 8077–8084. (d) Iwaoka, M.; Komatsu, H.; Tomoda, S. *Chem. Lett.* **1998**, 969–970. (e) Wirth, T.; Fragale, G.; Spichty, M. *J. Am. Chem. Soc.* **1998**, *120*, 3376–3381. (f) Komatsu, H.; Iwaoka, M.; Tomoda, S. *Chem. Commun.* **1999**, 205–206. (g) Spichty, M.; Fragale, G.; Wirth, T. *J. Am. Chem. Soc.* **2000**, *122*, 10914–10916. (h) Iwaoka, M.; Komatsu, H.; Katsuda, T.; Tomoda, S. *J. Am. Chem. Soc.* **2002**, *124*, 1902–1909. (i) Iwaoka, M.; Katsuda, T.; Tomoda, S.; Harada, J.; Ogawa, K. *Chem. Lett.* **2002**, 518–519. (j) Iwaoka, M.; Komatsu, H.; Katsuda, T.; Tomoda, S. *J. Am. Chem. Soc.* **2004**, *126*, 5309–5317. (k) Iwaoka, M.; Katsuda, T.; Komatsu, H.; Tomoda, S. *J. Org. Chem.* **2005**, *70*, 321–327. (l) Bayse, C. A.; Baker, R. A.; Ortwine, K. N. *Inorg. Chim. Acta* **2005**, *358*, 3849–3854. (m) Roy, D.; Sunoj, R. B. *J. Phys. Chem. A* **2006**, *110*, 5942–5947.

(21) Barton, D. H. R.; Hall, M. B.; Lin, Z.; Parekh, S. I.; Reibenspies, J. *J. Am. Chem. Soc.* **1993**, *115*, 5056–5059.

(22) Panda, A.; Menon, S. C.; Singh, H. B.; Butcher, R. J. *J. Organomet. Chem.* **2001**, *623*, 87–94.

(23) Panda, A.; Mugesh, G.; Singh, H. B.; Butcher, R. J. *Organometallics* **1999**, *18*, 1986–1993.

(24) The aerial oxidation of the telluride **21** to spirodiazatellurane (**25**) is not surprising, as the aerial oxidation of certain tellurides to spirodioxytellurane is well documented in the literature. For details, see ref 2a.

(25) Flack, H. *Acta Crystallogr., Sect. A* **1983**, *39*, 876–881.

(26) Although the racemic form of **25** was resolved spontaneously during the crystallization, a racemization was observed when the optically pure crystals were dissolved in organic solvents such as $CHCl_3$. The ^{125}Te NMR in the presence of chiral shift reagent indicated the presence of two enantiomers (Figure S31, Supporting Information).

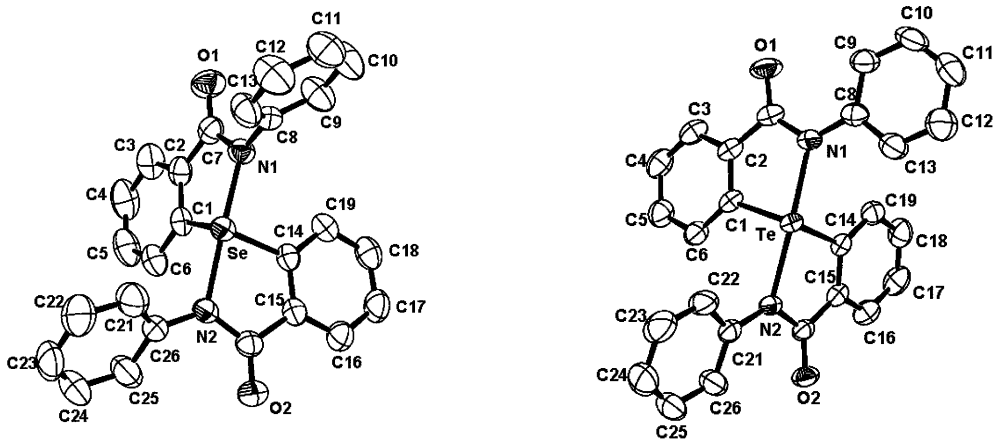

24 **25**

Figure 3. Single-crystal X-ray structures of compounds **24** and **25** (the solvent molecule, CH_2Cl_2 in **24** and Et_2O in **25**, and H atoms are omitted for clarity). Selected bond lengths (Å) and angles (deg) for **24**: Se−N1 = 2.024(2), Se−N2 = 2.058(2), Se−C1 = 1.938(3), Se−C14 = 1.929(3), N1−Se−N2 = 174.33(9), C1−Se−C14 = 11.34(13), C14−Se−N1 = 94.73(11), C14−Se−N2 = 81.70(10), C1−Se−N2 = 94.04(11), C1−Se−N1 = 82.30(11), N1−Se−N2 = 174.33(9). Selected bond lengths (Å) and angles (deg) for **25**: Te−N1 = 2.209(4), Te−N2 = 2.219(5), Te−C1 = 2.107(5), Te−C14 = 2.109(6), N1−Te−N2 = 163.73(17), C14−Te−N1 = 90.09(19), C14−Te−N2 = 78.6(2), C1−Te−C14 = 96.2(2), C1−Te−N2 = 91.32(17), C1−Te−N1 = 78.20(17).

Scheme 2. Selenide **26** Reacts with H_2O_2 to Yield Selenoxide **27**, Which Slowly Undergoes Hydrolysis and Spirocyclization to Produce the Spirodioxyselenurane **2**

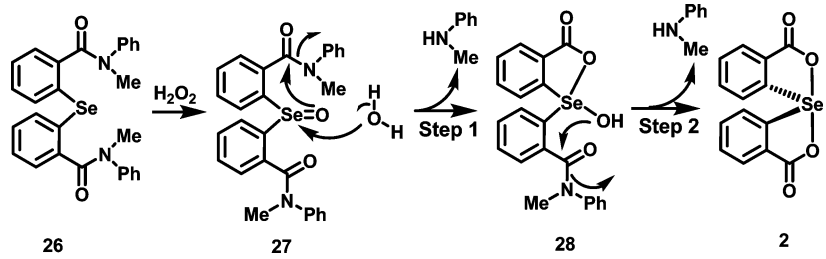

completely characterized by NMR and mass spectrometric techniques. Therefore, the mechanism for the formation of compounds **24** and **25** involves the initial oxidation of the selenide **20** and telluride **21** to produce the selenoxide (**22**) and telluroxide (**23**), respectively, which undergo dehydrocyclization reactions to produce the corresponding spiro compounds. It was observed that the presence of an excess amount of H_2O_2 does not affect the yield of **24** and **25**, as these compounds do not undergo any further reactions with H_2O_2.

Interestingly, selenoxide **27** underwent a very slow spirocyclization reaction to produce the spirodioxyselenurane **2** when the compound was kept in solution for a prolonged period (Scheme 2). The identity of compound **2** was unambiguously confirmed by single-crystal X-ray analysis. Although hydrolysis of amide bonds is extremely difficult, this unusual and unprecedented cyclization may occur via the initial attack of a water molecule at the selenium(IV) center followed by an attack of the selenium-bound oxygen atom at one of the amide carbonyl atoms to form a five-membered ring (Scheme 2, step 1). Subsequent attack of the selenium-bound hydroxyl group at the second amide carbonyl atom leads to the formation of the stable spirodioxyselenurane **2** (Scheme 2, step 2). On the basis of our theoretical studies of compound **22** (*vide infra*), it can be envisaged that the presence of Se···O interaction in compound **27** may facilitate the initial water attack at the selenium center, as these interactions are known to increase the electrophilic reactivity of the selenium center.[27]

Theoretical Investigation of Spirocyclization. The experimental observations suggested that the selenide (**20**) and telluride (**21**) react with H_2O_2 to produce the spirodiazaselenurane (**24**) and spirodiazatellurane (**25**) via selenoxide (**22**) and telluroxide (**23**) intermediates (Scheme 1). Further, the intermediacy of sulfoxides in the formation of spirosulfuranes from sulfides in the presence of H_2O_2 is well documented in the literature.[12] The fast cyclization of the telluride **21** to the spirodiazatellurane **25** in the presence of H_2O_2/t-BuOOH compared to that of the selenium analogue **20**, and the previous report for the requirement of dehydrating agents for the cyclization of sulfoxides to spiro compounds,[12] led us to investigate the spirocyclization mechanism by using the density functional theory (DFT) method. To find out the mechanism for the cyclization of E-oxide to spirochalcogenurane, we have carried out DFT calculations on the E-oxides **22**, **23**, and **29** to the corresponding spirodiazachalcogenuranes **24**, **25**, and **30**. The optimizations were carried out at the B3LYP level[28] using the LANL2DZdp ECP basis set[29] for S, Se, and Te and the 6-31G(d) basis set for all other atoms. Hereafter, we write the level of theory and basis sets together as B3LYP/6-31G(d)//LANL2DZdp ECP. The calculations reveal that the chalcogenoxides **22**, **23**, and **29** are stabilized by (i) an O···E intramolecular nonbonded interaction

(27) Sarma, B. K.; Mugesh, G. *J. Am. Chem. Soc.* **2005**, *127*, 11477–11485, and references therein.
(28) (a) Lee, C.; Yang, W.; Parr, R. G. *Phys. Rev. B* **1988**, *37*, 785–789. (b) Becke, A. D. *J. Chem. Phys.* **1993**, *98*, 5648–5652.
(29) (a) Hay, P. J.; Wadt, W. R. *J. Chem. Phys.* **1985**, *82*, 270–283. (b) Hay, P. J.; Wadt, W. R. *J. Chem. Phys.* **1985**, *82*, 284–298. (c) Hay, P. J.; Wadt, W. R. *J. Chem. Phys.* **1985**, *82*, 299–310. (d) Check, C. E.; Faust, T. O.; Bailey, J. M.; Wright, B. J.; Gilbert, T. M.; Sunderlin, L. S. *J. Phys. Chem. A* **2001**, *105*, 8111–8116.

Table 1. Structural Parameters and NBO Second-Order Perturbation Energy for the Chalcogenoxides and Some of Their Important Transition States and Intermediates Calculated at the B3LYP/6-31G(d)//LANL2DZdp ECP Level of Theory[a]

compound	$r_{E\cdots O}$ (Å)	∠O−E−O (deg)	∠O−E−N (deg)	E (kcal/mol)[b] $n_O\rightarrow\sigma^*_{E-O}$	E (kcal/mol)[b] $n_O\rightarrow\sigma^*_{E-N}$
22	2.786	171.9	123.2	4.71	
23	2.720	166.6	119.6	8.55	
29	2.931	173.3	126.5	0.65	
22TS1	2.936	124.4	158.1	0.70	
23TS1	2.700	157.6	119.9		11.3
29TS1	3.126	111.0	171.6		4.27
22INT1	2.829	96.2	172.3		11.3
23INT1	2.645	109.3	158.3		17.87
29INT1	2.968	91.2	178.1		0.85

[a] The details about basis sets are given in the Computational Methods. [b] NBO second-order perturbation energy is the summation of contributions from both the lone pairs of oxygen atoms.

between the chalcogen (E) atom and one of the amide oxygen atom and (ii) a hydrogen-bonding interaction of the chalcogenoxide (E═O) oxygen atom with the −NH− hydrogen atom of the neighboring amide group. Natural bond orbital (NBO) second-order perturbation energy analysis[30] at the B3LYP/6-31G(d)//LANL2DZdp ECP level of theory on **22**, **23**, and **29** suggests that the stabilization energy due to an $n_O\rightarrow\sigma^*_{E\text{-}O}$ orbital interaction ($E_{E\cdots O}$) increases in the order S < Se < Te (Table 1). Further, it was observed that the cyclization from E-oxide to spiro compound can take place in a stepwise manner involving two pathways: (i) pathway (a) is the kinetically favored one involving a high-energy distorted trigonal-bipyramidal intermediate (TBP) (e.g., **22INT2a**) in which the apical positions are occupied by the hydroxyl oxygen atom and a carbon atom of one of the phenyl rings. In this confirmation, the amide nitrogen atom, carbon atom of the other phenyl ring, and the lone pair of electrons on selenium occupy the equatorial positions. This high-energy TBP intermediates are subsequently converted to corresponding spiro compounds. (ii) Pathway (b) is the thermodynamically favored pathway, in which the high-energy TBP hydroxyl chalcogenurane intermediate is further converted to a more stable TBP intermediate (e.g., **22INT2b**). In this intermediate, the apical positions are occupied by the electronegative amide nitrogen atom and the oxygen atom of the −OH group with the two phenyl carbon atoms and the lone pair of electrons on selenium occupying the equatorial positions. The stable TBP intermediate then eliminates a water molecule to generate the spirodizachalcogenurane (Scheme 3).

Herein, we discuss both pathways (a) and (b) for the formation of the spirodiazaselenurane (**24**) and briefly provide a comparison of the energies with those of the sulfur (**30**) and tellurium (**25**) analogues. The optimized geometries of various intermediates and transition states (TS) involved in the cyclization reaction of selenoxide **22** to the corresponding spirodiazaselenurane **24** and the activation energy profile are shown in Figures 4 and 5, respectively. The relative electronic energies (ZPE corrected) and Gibbs free energy (ZPE corrected) in the gas phase for the cyclization of **22**, **23**, and **29** are summarized in Table 2. The nature of potential energy surfaces (PES) for the cyclization of **23** and **29** is similar to that of **22** as shown in Figure 5, and the cyclization can follow either pathway (a) or pathway (b).

In both pathways (a) and (b), the first ring closure reaction of the selenoxide **22** generates the distorted TBP hydroxyselenurane intermediate **22INT1** via the transition state **22TS1**, having an activation energy barrier of ∼45 kcal/mol (Table 2). In the transition state **22TS1**, a nucleophilic attack of one of the nitrogen atoms at the selenium center takes place and the oxygen atom attached to selenium abstracts the NH proton. In should be noted that the $n_O\rightarrow\sigma^*_{Se-O}$ orbital interaction is completely broken in this transition state (Table 1). In pathway (a), **22INT1** is converted to another intermediate, **22INT2a**, via another transition state (**22TS2a**), which has a very low activation energy barrier (1.94 kcal/mol). It should be noted that the apical positions of the TBP geometry around the selenium center in both **22INT1** and **22INT2a** intermediates are not occupied by electronegative atoms (∠N−Se−OH ≈ 90°). However, **22INT2a** adopts a geometry that can lead to elimination of a water molecule via the transition state **22TS3a**. As the transition state **22TS3a** is only 11.70 kcal/mol higher in energy than the hydroxyselenurane intermediate **22INT2a**, the second amide nitrogen atom in **22TS3a** can easily attack at the selenium center and the hydroxyl group can abstract the NH proton, leading to the elimination of a water molecule. In the transition state **22TS3a**, the Se−O bond is significantly elongated (2.40 Å) and the OH is strongly hydrogen bonded to the NH group (HO···HN = 1.51 Å). Furthermore, the nitrogen atom moves much closer to the selenium center (Se···N = 2.73 Å). In the overall process, the first step involving hydroxyselenurane formation is the rate-limiting one.

In pathway (b), the intermediate **22INT1**, produced from **22** via the transition state **22TS1**, is converted to a stable intermediate **22INT2b** via the transition state **22TS2b**.[31] In **22INT2b**, the apical positions of the TBP geometry around the selenium center are occupied by electronegative atoms (∠N−Se−OH ≈ 180°), and **22INT2b** is 15.25 kcal/mol more stable than **22INT1**. Furthermore, there is a −NH···OH hydrogen bond (1.83 Å) in **22INT2b**, which introduces the required geometrical arrangements for the second ring closure to form the spiro compound. Subsequently, **22INT2b** cyclizes to spiro compound **24** via transition state **22TS3b**, having an activation energy barrier of 24.92 kcal/mol. Although pathway (a) is a kinetically favored process, pathway (b) represents a thermodynamically more favored mechanism due to the higher stability of the intermedi-

Scheme 3. Stepwise Mechanism for the Formation of Spirodiazachalcogenuranes from Chalcogen Oxides via a Trigonal Bipyramidal (TBP) Intermediates

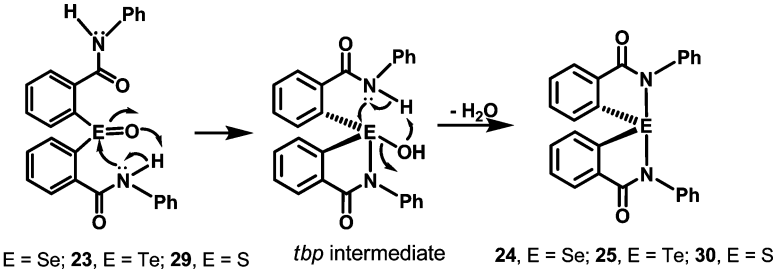

22, E = Se; **23**, E = Te; **29**, E = S *tbp* intermediate **24**, E = Se; **25**, E = Te; **30**, E = S

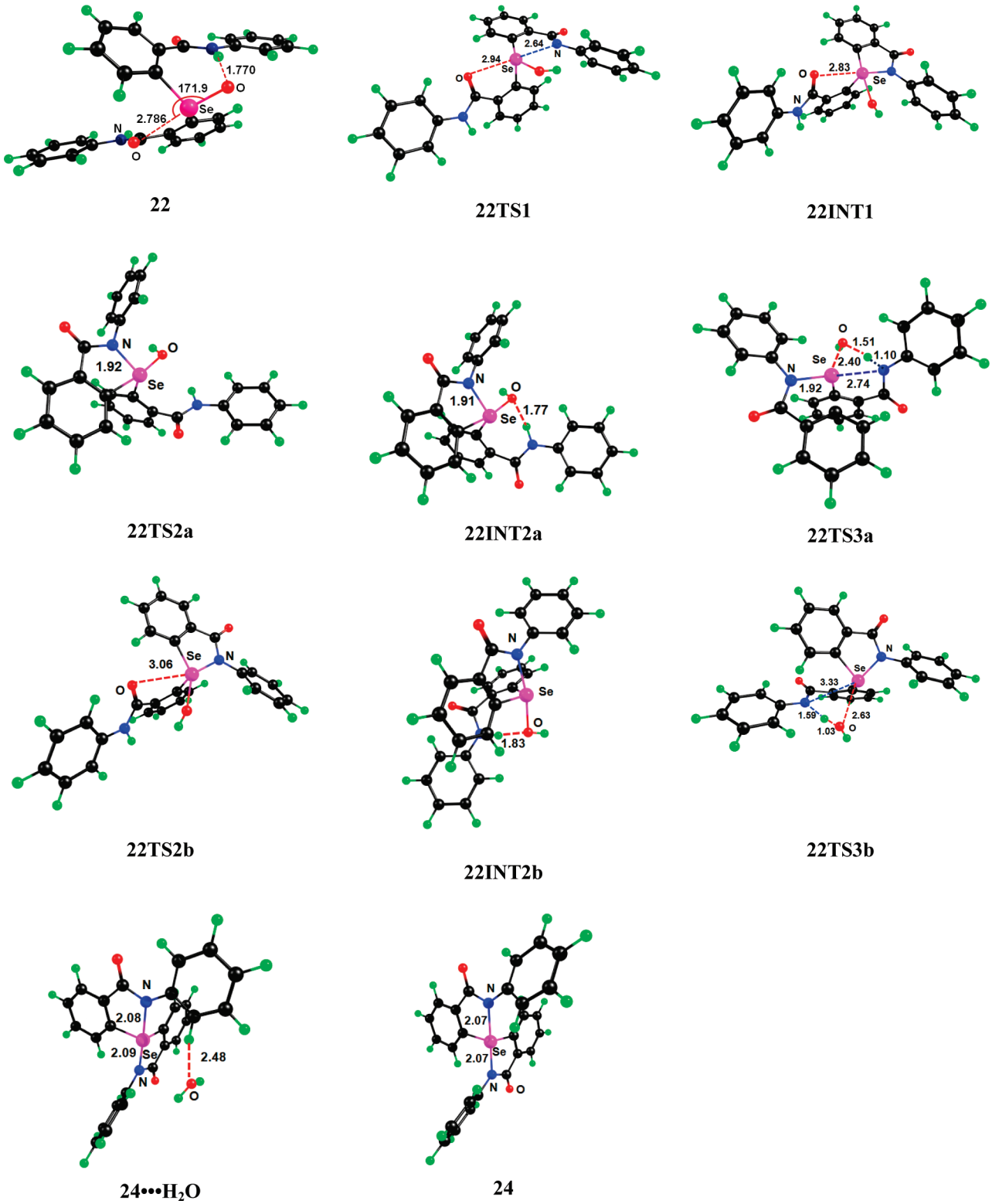

Figure 4. Optimized geometries of reactant, transition states, intermediates, and product involved in the spirocyclization of **22** to **24**.

ates. These two different pathways (a) and (b) were also observed for the sulfoxide (**29**) and telluroxide (**23**),[32] although considerable differences in the energy were observed for the intermediates and transition states.

Similar to the selenoxide **22**, the highest activation energy barrier is associated with the cyclization of the first ring, and therefore, this step becomes the rate-limiting step for the spirocyclization of the sulfoxide and telluroxide (Table 2). A comparison of the cyclization steps involving chalcogenoxides indicates that the activation energy barrier decreases in the order S > Se > Te. The most striking feature in the tellurium case is

(30) (a) Reed, A. E.; Curtiss, L. A.; Weinhold, F. *Chem. Rev.* **1988**, *88*, 899–926. (b) Glendening, E. D.; Reed, J. E.; Carpenter, J. E.; Weinhold, F. *NBO Program 3.1*; Madison, WI, 1988.

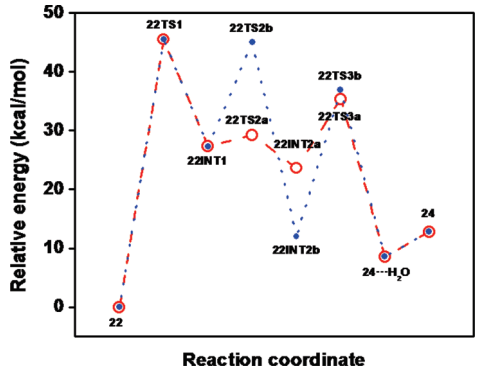

Figure 5. Energy profile for the stepwise conversion of selenoxide **22** to spirodiazaselenurane **24**. [Red dashed line represents pathway (a) and blue dotted line represents pathway (b).]

the shorter Te···O distance in **23TS1** compared to that of **23**. Although the $n_O \rightarrow \sigma^*_{Te-O}$ interaction is completely broken in **23TS1**, a new $n_O \rightarrow \sigma^*_{Te-N}$ (11.3 kcal/mol) interaction is generated (Table 1), which may contribute to stabilizing the transition state **23TS1**. It should be noted that no such interactions are present in **22TS1** and **29TS1** for selenium and sulfur, respectively. Similarly, the $n_O \rightarrow \sigma^*_{Te-N}$ interaction (17.87 kcal/mol) in the first intermediate (**23INT1**) is much higher than the interactions in the sulfur and selenium analogues **29INT1** (0.86 kcal/mol) and **22INT1** (4.27 kcal/mol), respectively. This difference may account for the higher stability of the tellurium intermediate (Table 1). As it can be seen from Table 2, the activation energy barriers are much lower for the telluroxide than the selenium and sulfur analogues, and formation of the spirodiazatellurane is a thermodynamically favored process (negative ΔG values). As a result, tellurium(II) compounds are more susceptible to aerial oxidation than their selenium and

Table 2. Relative Electronic ΔE (ZPE corrected) and Relative Gibbs Free Energy ΔG (ZPE corrected) for the Cyclization of **22**, **23**, and **29** to the Corresponding Spiro Compounds **24**, **25**, and **30** via Pathway (a) and (b) Calculated at the B3LYP/6-31G(d)//LANL2DZdp ECP Level of Theory

22 → 24 + H_2O

					22TS2a	**22INT2a**	**22TS3a**		
				a	ΔE	29.24	23.63	35.33	a
					ΔG	29.75	24.09	36.78	
	22	**22TS1**	**22INT1**						**[24•••H_2O]**	**[24 + H_2O]**
ΔE	0	45.49	27.30						8.58	12.81
ΔG	0	45.79	26.91	b				b	7.78	4.36
					22TS2b	**22INT2b**	**22TS3b**		
					ΔE	44.98	12.05	36.97	
					ΔG	45.14	13.16	38.23	

23 → 25 + H_2O

					23TS2a	**23INT2a**	**23TS3a**		
				a	ΔE	14.66	9.75	23.68	a
					ΔG	14.21	9.88	25.13	
	23	**23TS1**	**23INT1**						**[25•••H_2O]**	**[25 + H_2O]**
ΔE	0	26.47	10.36						0.24	4.99
ΔG	0	26.97	8.93	b				b	-0.63	-3.58
					23TS2b	**23INT2b**	**23TS3b**	**23INT3b**	**23TS4b**	
				ΔE	25.0	5.92	5.92	1.55	25.89	
				ΔG	26.19	5.28	6.64	4.23	-27.72	

29 → 30 + H_2O

					29TS2a	**29INT2a**	**29TS3a**		
				a	ΔE	42.96	36.51	39.12	a
					ΔG	44.06	37.10	39.50	
	29	**29TS1**	**29INT1**						**[30•••H_2O]**	**[30 + H_2O]**
ΔE	0	58.67	42.53						8.58	12.81
ΔG	0	58.57	42.38	b				b	7.78	4.36
					29TS2b	**29INT2b**	**29TS3b**		
					ΔE	62.85	25.34	46.17	
					ΔG	63.85	26.61	47.37	

Table 3. Initial Rates (v_0) and $t_{1/2}$ Values for the Reduction of t-BuOOH by BnSH in the Presence of Various Selenium and Tellurium Compounds

compound	v_0 (μM/min)[a]	$t_{1/2}$ (h)[a]
control	0.10 ± 0.01	97
ebselen	0.11 ± 0.01	79
20	0.10 ± 0.01	88
21	27.64 ± 1.24	1.7
24	2.00 ± 0.11	62
25	1.77 ± 0.01	4.8

[a] The reactions were carried out in CH_2Cl_2/MeOH (95:5); BnSH, 5 mM; t-BuOOH, 7 mM; catalyst, 0.5 mM,; temperature, 23 °C.

sulfur counterparts. The higher susceptibility to aerial oxidation together with a low activation energy barrier and negative ΔG values for the cyclization reaction correlate well with our experimental observation that the telluride **21** undergoes a spontaneous spirocyclization to produce **25** in solution even in the absence of any oxidizing agent. Further, the computed activation energies clearly support the experimental observations that the cyclodehydration reaction in the chalcogenoxides occurs spontaneously for selenium and tellurium, whereas for sulfur it requires a dehydrating agent.

Glutathione Peroxidase (GPx)-like Antioxidant Activity. Despite their stability in different solvents, compounds **24** and **25** reacted readily with thiols such as thiophenol (PhSH) and benzyl thiol (BnSH) to produce the selenide **20** and telluride **21**, respectively, in quantitative yield. The reactions of **20** and **21** with H_2O_2/t-BuOOH to produce the corresponding spiro compounds (**24**, **25**) and the facile cleavage of the Se/Te−N bond in **24** and **25** by thiols led us to investigate their glutathione peroxidase activity. The GPx-like catalytic activity was studied by a reverse-phase HPLC method using aqueous t-BuOOH as substrate and BnSH as co-substrate.[15,17a,33] The initial rates (v_0) for the reduction of peroxide by BnSH in the presence and absence of catalyst were calculated (Table 3), and the rates were compared to that of ebselen (2-phenyl-1,2-benzisoselenazol-3(2*H*)-one), a well-known GPx mimic that exhibits interesting antioxidant and anti-inflammatory activities.[34] Compounds **20**, **21**, **24**, and **25** were also evaluated for their ability to catalyze at least 50% conversion of the thiol (BnSH) to disulfide (BnSSBn) in the presence of t-BuOOH by following the method reported by Back and co-workers.[15,17a,29]

In agreement with the previous reports,[15,17a,33] ebselen exhibits moderate activity in the reduction of t-BuOOH in the presence of BnSH as the thiol cofactor (Table 3). The activity of selenide **20** is almost identical to that of ebselen. The $t_{1/2}$ value determined for the spirodiazaselenurane **24** is about 1.4 times smaller than that of **20**, although the initial rate observed for **24** is almost 20 times higher than that of **20**. This is due to the facile cleavage of the Se−N bond in **24** by BnSH, which leads to a steady increase in the formation of BnSSBn during the initial period of the reaction. However, the $t_{1/2}$ value indicates that the oxidation of the selenium center in selenide **20** is rather slow, and therefore, the rate decreases when **24** is completely converted to selenide **20** (Figure S32, Supporting Information). These observations also indicate that the spirodiazaselenurane **24** is not regenerated during the catalytic cycle. Therefore, the observed catalytic activity of compound **24** is mainly due to a redox shuttle between selenide **20** and selenoxide **22**.[35]

Scheme 4. Proposed Catalytic Mechanism for the Reduction of Peroxide by Thiols in the Presence of Spirodiazatellurane **25**

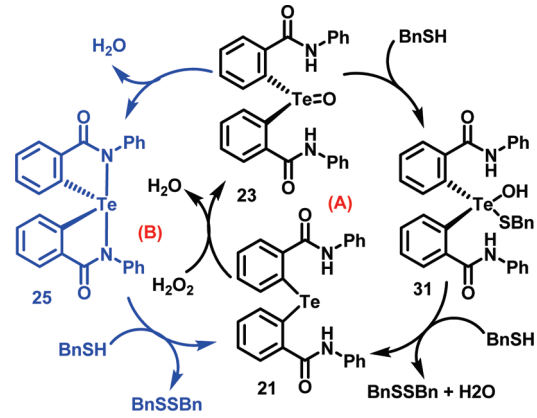

In contrast to the selenide **20**, the tellurium analogue (**21**) exhibited very high catalytic activity, and the initial rate observed for **21** was about 250 times higher than that of ebselen. The $t_{1/2}$ value for this compound (~1.7 h) was also found to be much lower than that of ebselen (79 h) and selenide **20** (88 h). A comparison of the catalytic activity of the spirodiazatellurane **25** to that of the selenium analogue **24** leads to some interesting observations. While the rate of conversion of **24** to **20** (v_0: 0.53 μM/min) is almost identical to that of **25** to **21** (v_0: 0.47 μM/min) in the presence of BnSH, the oxidation of the tellurium center in **21** is much faster than that of the selenium center in **20**. As a result, the catalytic activity of **25** increases after the formation of the telluride **21**. This leads to a redox cycle involving the telluride **21** and telluroxide **23** (Scheme 4, cycle A), which accounts for most of the catalytic activity. However, the spirodiazatellurane **25** becomes the predominant species at lower concentration of thiol and higher concentration of peroxide. In fact, compound **25** disappeared completely only when a large excess of thiol (10 equiv or more) was used. This type of reversible spirocyclization (Scheme 4, cycle B) is important, as the cyclization may protect the tellurium moiety from conversion to other oxidized compounds such as Te(VI) species, particularly at higher concentrations of peroxides, which may significantly reduce the catalytic applications. It should be noted that although some aliphatic spirodioxyselenuranes and spirodioxytelluranes are known to have higher activity than that of **25**, aromatic spirochalcogenuranes have been shown to be poor catalysts.

(31) It should be noted that in the case of tellurium one more intermediate (**23INT2b**) was observed between the first intermediate (**23INT1**) and the stable intermediate having ∠N−Se−OH ≈ 180° (**23INT3b**) (Table 2). However, this intermediate (**23INT2b**) converts to **23INT3b** via transition state **23TS3b**, having no activation energy barrier. Therefore, it is not surprising that we have not observed any such intermediates in the case of sulfur and selenium.

(32) For tellurium, repeated attempts to find out the transition state connecting **23INT3b** and **25**···**H$_2$O** failed, and every time the transition state optimization converged to the transition state **23TS3a** of pathway (a) water elimination was involved. Further, we observed that **23INT3b** converts to **23INT2a** via transition state **23TS4b**. This indicates that pathway (b) merges with pathway (a) and pathway (a) is the one that leads to the formation of a spiro compound.

(33) (a) Back, T. G.; Moussa, Z. *J. Am. Chem. Soc.* **2002**, *124*, 12104–12105. (b) Back, T. G.; Moussa, Z. *J. Am. Chem. Soc.* **2003**, *125*, 13455–13460.

(34) (a) Sies, H.; Masumoto, H. *Adv. Pharmacol.* **1997**, *38*, 229–246. (b) Mugesh, G.; Singh, H. B. *Chem. Soc. Rev.* **2000**, *29*, 347–357. (c) Mugesh, G.; du Mont, W.-W.; Sies, H. *Chem. Rev.* **2001**, *101*, 2125–2179, and references therein. (d) Noguira, C. W.; Zeni, G.; Rocha, J. B. T. *Chem. Rev.* **2004**, *104*, 6255–6286.

(35) It should be noted that the lower $t_{1/2}$ for **24** (62 h) as compared to that of **20** (88 h) is not because of the regeneration of **24** in the catalytic cycle, but is due to the initial ~20% conversion of BnSH to BnSSBn, which arises from the direct reaction of BnSH with **24** during the first ~140 min.

Peroxynitrite (PN) Scavenging Activity. The high GPx activity of telluride **21** and the spiro compound **25** led us to investigate the effect of these compounds on PN-mediated oxidation reactions. It is known that diaryl selenides and diaryl tellurides inhibit oxidation and nitration reactions mediated by PN and themselves oxidize to selenoxides and telluroxides, respectively.[36,37] The PN-mediated oxidation of dihydrorhodamine 123 (DHR) to rhodamine 123 was studied by fluorescence spectroscopy, and the effect of these selenium and tellurium compounds in the oxidation reaction were compared to that of ebselen, which scavenges PN effectively with a second-order rate constant of 2×10^6 M^{-1} s^{-1}.[38] The ability of selenium and tellurium compounds to inhibit the PN-mediated reaction is represented by their IC_{50} values. As expected, ebselen inhibited the DHR to rhodamine conversion with an IC_{50} value of 0.96 ± 0.01 μM (Table 4). The diaryl selenide **20** exhibited a weak inhibition with an IC_{50} value of 71.96 ± 1.30 μM. As previously mentioned, compound **20** is also a poor catalyst in the reduction of peroxides by thiols. These observations indicate that the oxidation of selenide **20** to the corresponding selenoxide **22** is an extremely slow process. In agreement with our observations on the reactivity of spirodiazaselenurane (**24**) and spirodiazatellurane (**25**) toward H_2O_2, these compounds did not show any noticeable effect on the PN-mediated oxidation. This indicates that the selenium or tellurium center does not undergo further oxidation to produce any Se(VI) or Te(VI) species. In contrast to the selenide **20** and spiro compounds **24** and **25**, the telluride **21** exhibited very strong inhibition, with IC_{50} values of 1.92 ± 0.02 μM, which clearly indicates that the tellurium center in **21** is rapidly oxidized by PN. This is also in agreement with our observation that the telluride **21** exhibits good GPx-like activity due to the facile oxidation in the presence of H_2O_2/t-BuOOH.

Table 4. IC_{50} Values for the Inhibition of PN-Mediated Oxidation of Dihydrorhodamine 123 by Ebselen, **20** and **21**[a]

compound	IC_{50} (μM)
ebselen	0.96 ± 0.01
20	71.96 ± 1.30
21	1.92 ± 0.02

[a] Conditions: dihydrorhodamine 0. 5 μM; peroxynitrite 1.0 μM; 100 mM sodium phosphate buffer having 100 μM DTPA; pH 7.4; variable concentrations of inhibitors.

Conclusions

In summary, we have described the synthesis, structural features, and thiol peroxidase activity of stable spirodiazaselenuranes and spirodiazatelluranes bearing benzanilide moieties. This study indicates that although 2,2′-selenobis(benzamide) does not produce any spirodiaza compound upon oxidation by H_2O_2, the replacement of the $-NH_2$ group in 2,2′-selenobis-(benzamide) by a $-$NHPh moiety helps in stabilizing spirodiazaselenurane. The crystal structure of the spirodiazaselenurane **24** and spirodiazatellurane **25** suggested distorted trigonal-bipyramidal (TBP) geometries around the chalcogen atom, the geometry around the tellurium center in **25** being more distorted. The tellurium compound **25** underwent a spontaneous chiral resolution during crystallization to give the first example of chiral spirodiazachalcogenurane. When the cyclization reaction leading to spiro compounds was blocked by replacing the free $-$NH$-$ hydrogen atom with alkyl groups, the selenide reacted with H_2O_2 to produce the corresponding selenoxide. Furthermore, the telluroxide **23** can be detected by low-temperature ^{125}Te NMR studies. These observations suggest that the spirocyclization reactions of selenide **20** and telluride **21** take place via the involvement of selenoxide **22** and telluroxide **23**. DFT calculations on the spirocyclization of the chalcogenoxides suggested two pathways, both of which follow stepwise mechanisms involving hydroxyl chalcogenurane intermediates. The activation energy barrier for the spirocyclization was found to be much lower for the telluroxide **23** than its sulfur and selenium analogues, which clearly supports our experimental observation that the spirocyclization of telluride in solution takes place even in the absence of an oxidizing agent. While the spirodiazaselenurane exhibits a GPx-like activity similar to that of ebselen, the tellurium analogue exhibits a remarkably high catalytic activity.[39] This is due to the involvement of an efficient redox cycle between the telluride and telluroxide. At low thiol concentrations, the telluroxide undergoes a reversible spirocyclization, which may protect the tellurium moiety from overoxidation. The telluride was also found to be an efficient scavenger of peroxynitrite. The selenium and tellurium compounds reported in this paper represent a novel class of catalyst for the reduction of harmful peroxides by thiols.

Experimental Section

General Procedures. *n*-Butyllithium (n-BuLi) was purchased from Acros Chemical Co. (Belgium). Selenium and tellurium dioxides were obtained from Aldrich Chemical Co. All other chemicals were of the highest purity available. All experiments were carried out under anhydrous and anaerobic conditions using standard Schlenk techniques for the synthesis. Due to unpleasant odors of several of the reaction mixtures involved, most manipulations were carried out in a well-ventilated fume hood. Mass spectral (MS) studies were carried out on a Q-TOF Micro mass spectrometer with electrospray ionization MS mode analysis. In the case of isotopic patterns, the value given is for the most intense peak. Liquid state NMR spectra were recorded in $CDCl_3$, d_4-MeOH, or d_6-DMSO as a solvent. ^{1}H (400 MHz) and ^{13}C (100 MHz) NMR spectra were obtained on a Bruker Avance 400 NMR spectrometer using the solvent as an internal standard for ^{1}H and ^{13}C. Chemical shifts (^{1}H, ^{13}C) are cited with respect to tetramethylsilane (TMS). Thin-layer chromatography analyses were carried out on precoated silica gel plates (Merck), and spots were visualized by UV irradiation. Column chromatography was performed on glass columns loaded with silica gel or on an automated flash chromatography system (Biotage) by using preloaded silica cartridges. High-performance liquid chromatography (HPLC) experiments were carried out on a Waters Alliance System (Milford, MA) consisting of a 2695 separation module, a 2996 photodiode-array detector, and a fraction collector. The assays were performed in 1.8 mL sample vials, and a built-in autosampler was used for sample injection. The Alliance HPLC System was controlled with EMPOWER software (Waters

(36) Andersson, C. M.; Hallberg, A.; Brattsand, R.; Cotgreave, I. A.; Engman, L.; Persson, J. *Bioorg. Med. Chem. Lett.* **1993**, *3*, 2553–2558.
(37) Giles, G. I.; Fry, F. H.; Tasker, K. M.; Holme, A. L.; Peers, C.; Green, K. N.; Klotz, L.-O.; Sies, H.; Jacob, C. *Org. Biomol. Chem* **2003**, *1*, 4317–4322.
(38) Masumoto, H.; Kissner, R.; Koppenol, W. H.; Sies, H. *FEBS Lett.* **1996**, *398*, 179–182.

(39) It should be noted that the tellurium analogue of ebselen (ebtellur) is not known, although ebtellur has been used as a model compound for computational studies to understand the reactivity of organotellurium compounds toward reactive oxygen species such as peroxynitrite. Therefore, the spiro analogue of ebtellur (**25**) may help clarify the effect of tellurium substitution in cyclic selenazole-based compounds. For theoretical studies on ebtellur and related compounds, see: (a) Sakimoto, Y.; Hirao, K.; Musaev, D. G. *J. Phys. Chem. A* **2003**, *107*, 5631–5639. (b) Musaev, D. G.; Hirao, K. *J. Phys. Chem. A* **2003**, *107*, 9984–9990.

Corporation, Milford, MA). $Se(dtc)_2$ and $Te(dtc)_2$ were synthesized by using literature methods.[40]

HPLC Assay. In this assay, we employed a mixture containing a 1:1.4 molar ratio of BnSH and t-BuOOH in dichloromethane/methanol (95:5) at room temperature as our model system. Runs with and without 10 mol % added test compounds were carried out under the same conditions. Periodically, aliquots were removed and the concentrations of the product BnSSBn were determined from the detector response, using pure BnSSBn as an external standard. The initial rates (v_0) for the conversion of thiols to the corresponding disulfides were calculated from the first 5% of the reactions, and the amounts of disulfide formed in these reactions were determined from the calibration plots of authentic disulfide.

Synthesis of Peroxynitrite (PN). Peroxynitrite was synthesized by following the literature method with minor modifications.[41] A solution of 30% (~8.82 M) H_2O_2 (5.7 mL) was diluted to 50 mL with water, chilled to about 4 °C in an ice/water mixture, added to 30 mL of 5 N NaOH and 5 mL of 0.04 M DPTA in 0.05 N NaOH with gentle mixing, and then diluted to a total volume of 100 mL. The concentration of H_2O_2 in the final solution was 0.5 M with a pH = 12.5−13.0. The buffered H_2O_2 was stirred vigorously with an equimolar amount of isoamyl nitrite (6.7 mL, 0.05 M) for 3−4 h at 25 °C. The reaction was monitored by withdrawing aliquots at intervals of 30 min and assaying for peroxynitrite at 302 nm by a UV−vis spectrophotometer. When the yield of peroxynitrite reached a maximum, the aqueous layer was washed with 3 × 2 volumes of dichloromethane, chloroform, or hexane in a separatory funnel to remove the excess isoamyl alcohol and isoamyl nitrite. The unreacted H_2O_2 was then removed by passing the aqueous phase through a column filled with 25 g of granular MnO_2. The solution was 500 times diluted with 0.1 N NaOH solution, and the concentration of peroxynitrite was measured at 302 nm ($\varepsilon = 1670$ M^{-1} cm^{-1}) by the UV−vis spectrophotometric method.

Peroxynitrite-Mediated Oxidation Assay. Peroxynitrite-mediated oxidation of dihydrorhodamine 123 (DHR) was followed as suggested in the literature with minor modifications.[41] Fluorescence intensity was measured using a Perkin-Elmer LS 50B luminescence spectrometer with excitation and emission wavelengths of 500 and 526 nm, respectively. The stock solution of DHR in dimethylformamide (DMF) was purged with nitrogen and stored at −20 °C. The working solutions of DHR and peroxynitrite were kept on an ice bath. The assay mixture contained DHR (0.50 μM) and peroxynitrite (1.0 μM) in 100 mM sodium phosphate buffer of pH 7.4 with 100 μM DTPA and variable inhibitor concentrations. The fluorescence intensity from the reaction of DHR with PN was set as 100%, and the intensity after the addition of various inhibitor amounts was expressed as the percentage of that observed in the absence of inhibitors. The final fluorescence intensities were corrected for background reactions. The inhibition plots were obtained using Origin6.1 software, and these plots were used for calculating the IC_{50} values of different inhibitors.

Synthesis of 20. To a stirred solution of benzanilide (1.0 g, 5.1 mmol) in dry THF (35 mL) under nitrogen at 0 °C was added *n*-BuLi (6.4 mL, 10.2 mmol, 1.6 M solution in hexane). After 30 min $Se(dtc)_2$ (0.98 g, 2.5 mmol) was added to the orange-red solution while a brisk stream of nitrogen was passed through the open system. The solution was stirred for 12 h at 25 °C, poured into a beaker containing 100 mL of cold water, and then extracted with dichloromethane. The dichloromethane extract was then evaporated under reduced pressure to give a yellow oil, which was then purified by flash chromatography using petroleum ether/ethyl acetate as eluent to give **20** as a white solid in 40% yield: ^{1}H NMR (DMSO-d_6) δ 10.43 (s, 1H), 7.67−7.71 (m, 3H), 7.44−7.30 (m, 5H), 7.36−7.41 (m, 3H), 7.08 (t, J = 8.0 Hz, 1H); ^{13}C NMR (DMSO-d_6) δ 167.2, 139.5, 139.4, 134.5, 132.3, 131.3, 129.1, 128.6, 127.7, 124.2, 120.4; ^{77}Se (DMSO-d_6) δ 417; HRMS (TOF MS ES$^+$) m/z 495.0588 [M + Na]$^+$.

Synthesis of 21. To a stirred solution of benzanilide (1.0 g, 5.1 mmol) in dry THF (35 mL) under nitrogen at 0 °C was added n-BuLi (6.4 mL, 10.2 mmol, 1.6 M solution in hexane). After 30 min $Te(dtc)_2$ (1.1 g, 2.5 mmol) was added to the orange-red solution while a brisk stream of nitrogen was passed through the open system. The solution was stirred for 12 h at 25 °C, poured into a beaker containing 100 mL of cold water, and then extracted with dichloromethane. The dichloromethane extract was then evaporated under reduced pressure to give a yellow oil, which was then purified by flash chromatography using petroleum ether/ethyl acetate as eluent to give **21** as a light yellow solid in 15% yield: ^{1}H NMR ($CDCl_3$) δ 7.77 (d, 2H, NH proton and the doublet of an aromatic proton merged together), 7.71 (d, J = 8.0 Hz, 1H), 7.45 (d, J = 8.0 Hz, 1H), 7.40 (t, J = 8.0 Hz, 1H), 7.30 (t, J = 8.0 Hz, 2H), 7.12 (t, J = 8.0 Hz, 1H); ^{13}C NMR ($CDCl_3$) δ 167.4, 139.0, 137.6, 131.6, 129.0, 127.8, 127.6, 124.7, 121.8, 120.3; ^{125}Te ($CDCl_3$) δ 716; HRMS (TOF MS ES$^+$) m/z 561.1558 [M + K]$^+$.

Synthesis of 24. To a stirred solution of **20** (200 mg, 0.42 mmol) in CH_2Cl_2 (10 mL) was added hydrogen peroxide (145 μL, 1.27 mmol). The reaction mixture was stirred for 20 h at 25 °C and the solvent was evaporated to dryness and purified by flash chromatography using petroleum ether/ethyl acetate as eluent to give the **24** as a white solid in 98% yield. ^{1}H NMR ($CDCl_3$) δ 8.28 (d, J = 8.0 Hz, 1H), 7.88 (d, J = 8.0 Hz, 1H), 7.69−7.73 (m, 3H), 7.63 (t, J = 8.0 Hz, 1H), 7.41 (t, J = 8.0 Hz, 2H), 7.19 (t, J = 8.0 Hz,1H); ^{13}C NMR ($CDCl_3$) δ 164.6, 140.5, 135.6, 135.4, 133.9, 133.1, 129.9, 129.7, 126.5, 125.3, 123.4. ^{77}Se ($CDCl_3$) δ 570; MS (TOF MS ES$^+$) m/z 471.0613 [M + H]$^+$.

Synthesis of 25. To a stirred solution of benzanilide (1.0 g, 5.1 mmol) in dry THF (35 mL) under nitrogen at 0 °C was added *n*-BuLi (6.4 mL, 10.2 mmol, 1.6 M solution in hexane). After 30 min $Te(dtc)_2$ (1.1 g, 2.5 mmol) was added to the orange-red solution while a brisk stream of nitrogen was passed through the open system. The solution was stirred for 12 h at 25 °C, poured into a beaker containing 100 mL of cold water, and then extracted with dichloromethane. The dichloromethane extract was then evaporated under reduced pressure to give a yellow oil, which was then purified by flash chromatography using petroleum ether/ethyl acetate as eluent to give **25** as a white solid in 40% yield: ^{1}H NMR ($CDCl_3$) δ 8.28 (dd, J = 7.6 and 1.6 Hz, 1H), 7.83 (d, J = 7.6 and 1.6 Hz, 1H), 7.62−7.71 (m, 4H), 7.44 (t, J = 8.0 Hz, 2H), 7.22 (t, J = 7.2 Hz, 1H); ^{13}C NMR ($CDCl_3$) δ 167.4, 141.6, 138.2, 134.1, 132.7, 130.9, 129.8, 127.9, 125.2, 124.3; ^{125}Te ($CDCl_3$) δ 742; HRMS (TOF MS ES$^+$) m/z 543.0299 [M + Na]$^+$.

Synthesis of 26. To a stirred solution of benzanilide (1.0 g, 5.1 mmol) in dry THF (35 mL) under nitrogen at 0 °C was added n-BuLi (6.4 mL, 10.2 mmol, 1.6 M solution in hexane). After 30 min $Se(dtc)_2$ (0.98 g, 2.5 mmol) was added to the orange-red solution while a brisk stream of nitrogen was passed through the open system. The solution was stirred for 2 h at 25 °C, methyl iodide (5.1 mmol) was added, and the reaction mixture was stirred for 12 h at 25 °C. The reaction mixture was then poured into a beaker containing 100 mL of cold water and then extracted with dichloromethane. The dichloromethane extract was then evaporated under reduced pressure to give a yellow oil, which was then purified by flash chromatography using petroleum ether/ethyl acetate as eluent to give **26** as a white solid in 40% yield: ^{1}H NMR ($CDCl_3$) δ 6.98−7.18 (m, 18H), 3.49 (s, 6H); ^{13}C NMR ($CDCl_3$) δ 169.1, 142.7, 138.8, 133.0, 129.1, 128.4, 128.0, 127.2, 126.0, 125.8, 125.6, 36.7; ^{77}Se ($CDCl_3$) δ 394; HRMS (TOF MS ES$^+$) m/z 523.0924 [M + Na]$^+$.

Synthesis of 27. To a stirred solution of **26** (100 mg, 0.2 mmol) in $CHCl_3$ (5 mL) at 25 °C was added aqueous hydrogen peroxide (30% v/v, 68 μL, 0.6 mmol, 8.82 M solution in water). After 12 h the solvent was evaporated under reduced pressure and the product was purified by flash chromatography using petroleum ether/ethyl acetate/MeOH as eluent to give **27** as a white solid in 85% yield:

(40) Foss, O. *Inorg. Synth.* **1953**, *4*, 88–93.
(41) Di Mascio, P.; Bechara, E. J. H.; Medeiros, M. H. G.; Briviba, K.; Sies, H. *FEBS Lett.* **1994**, *355*, 287–289.

^{1}H NMR ($CDCl_3$) δ 7.90 (d, J = 4.0 Hz, 2H), 7.38 (t, J = 8.0 Hz, 2H), 7.16−7.27 (m, 10H), 7.08 (t, J = 8.0 Hz, 2H), 6.96 (d, J = 4.0 Hz, 2H), 3.56 (s, 6H); ^{13}C NMR ($CDCl_3$) δ 168.2, 145.7, 144.5, 134.7, 130.8, 129.5, 129.4, 129.1, 127.9, 126.9, 126.8, 38.9; ^{77}Se ($CDCl_3$) δ 871; HRMS (TOF MS ES$^+$) m/z 539.0851 $[M + K]^+$.

Computational Methods

All calculations were performed using the Gaussian03 suite of quantum chemical programs.[42] The hybrid Becke 3-Lee−Yang−Parr (B3LYP) exchange correlation functional was applied for DFT calculations.[28] Geometries were fully optimized at the B3LYP level of theory by using the LANL2DZdp ECP basis set[29] for S, Se, and Te and the 6-31G(d) basis set for all other atoms. Transition states were searched by using the TS keyword. Furthermore, the transition state and the stable conformers were characterized by the presence or absence of a single imaginary mode. In all cases intrinsic reaction coordinate (IRC)[43] calculations were performed to confirm that the transition states connect the reactant and the product molecules. The activation energies are the difference in the zero-point vibrational energy (ZPVE) corrected electronic energy between the transition state and the stable conformations.

X-ray Crystallography. X-ray crystallographic studies were carried out on a Bruker CCD diffractometer with graphite-monochromatized Mo Kα radiation (λ = 0.71073 Å) controlled by a Pentium-based PC running the SMART software package.[44] Single crystals were mounted at room temperature on the ends of glass fibers, and data were collected at room temperature. The structures were solved by direct methods and refined using the SHELXTL software package.[45] All non-hydrogen atoms were refined anisotropically, and hydrogen atoms were assigned idealized locations. Empirical absorption corrections were applied to all structures using SADABS.[46,47] The structures were solved by direct methods (SIR-92) and refined by full-matrix least-squares procedures on F^2 for all reflections (SHELXL-97).

Crystal data for 20: $C_{26}H_{20}N_2O_2Se$; M_r = 471.4, monoclinic $C2/c$, a = 24.0692(30) Å, b = 5.1082(6) Å, c = 17.4862(22) Å, β = 108.292(2)°, V = 2041.30(15) Å^3, Z = 4, ρ_{calcd} = 1.53 g/cm, Mo Kα radiation (λ = 0.71073 Å), T = 293(2) K; R_1 = 0.036, wR_2 = 0.088 ($I > 2\sigma(I)$); R_1 = 0.047, wR_2 = 0.093 (all data).

Crystal data for 24: $C_{27}H_{20}Cl_2N_2O_2Se$; M_r = 554.3, monoclinic, space group $P2(1)/n$, a = 9.9821(32) Å, b = 22.9649(73) Å, c = 11.0534(36) Å, β = 105.729(5); V = 2438.98(38) Å^3, Z = 4, ρ_{calcd} = 1.51 g/cm, Mo Kα radiation (λ = 0.71073 Å), T = 293(2) K; R_1 = 0.038, wR_2 = 0.078 ($I > 2\sigma(I)$); R_1 = 0.065, wR_2 = 0.090 (all data).

Crystal data for 25 (racemic): $C_{28}H_{18}N_2O_{2.5}Te$; M_r = 550.1, triclinic, space group $P\bar{1}$, a = 10.8793(25) Å, b = 11.2653(28) Å, c = 11.4877(28) Å, α = 106.488(4)°; β = 114.488(5)°; γ = 94.871(5)°, V = 1195.03(46) Å^3, Z = 2, ρ_{calcd} = 1.53 g/cm, Mo Kα radiation (λ = 0.71073 Å), T = 293(2) K; R_1 = 0.046, wR_2 = 0.110 ($I > 2\sigma(I)$); R_1 = 0.060, wR_2 = 0.117 (all data).

Crystal data for 25 (*R*-enantiomer): $C_{26}H_{18}N_2O_2Te$; M_r = 518.0, orthorhombic, space group $P2_12_12_1$, a = 9.9216(10) Å, b = 10.6161(10) Å, c = 19.8643(19) Å, V = 2092.28(4) Å^3, Z = 4, ρ_{calcd} = 1.64 g/cm, Mo Kα radiation (λ = 0.71073 Å), T = 293(2) K; R_1 = 0.043, wR_2 = 0.064 ($I > 2\sigma(I)$); R_1 = 0.065, wR_2 = 0.072 (all data).

Crystal data for 25 (*S*-enantiomer). $C_{26}H_{18}N_2O_2Te$; M_r = 518.0, orthorhombic, space group $P2_12_12_1$, a = 9.9919(6) Å, b = 10.6098(6) Å, c = 19.8677(12) Å, V = 2093.57(2) Å^3, Z = 4, ρ_{calcd} = 1.64 g/cm, Mo Kα radiation (λ = 0.71073 Å), T = 293(2) K; R_1 = 0.058, wR_2 = 0.088 ($I > 2\sigma(I)$); R_1 = 0.093, wR_2 = 0.099 (all data).

Acknowledgment. This study was supported by the Department of Science and Technology (DST), New Delhi, and the Kitasato University Grant for International Exchange Programmes. We acknowledge the Supercomputer Education and Research Centre, Indian Institute of Science, for computing facilities. We thank Dibyendu Mallick and Dr. Mausumi Goswami for their help in theoretical calculations. G.M. acknowledges the DST for the award of Ramanna and Swarnajayanti fellowships.

Supporting Information Available: ^{1}H, ^{13}C, ^{77}Se, and ^{125}Te NMR spectra, ESI mass spectra, HPLC traces, archive entries for the optimized geometries, and the full reference of ref 42. This material is available free of charge via the Internet at http://pubs.acs.org.

JA908080U

(42) *Gaussian 03, Revision C.02*; Gaussian, Inc.: Wallingford, CT, 2004. The full reference is given in the Supporting Information.
(43) Fukui, K. *Acc. Chem. Res.* **1981**, *14*, 363–368.
(44) *SMART, Version 5.05*; Bruker AXS: Madison, WI, 1998.
(45) Altomare, A.; Cascarano, G.; Giacovazzo, C.; Gualardi, A. *J. Appl. Crystallogr.* **1993**, *26*, 343–350.
(46) Sheldrick, G. M. *Acta Crystallogr., Sect. A* **1990**, *46*, 467–473.
(47) Sheldrick, G. M. *SHELX-97, Program for the Refinement of Crystal Structures*; University of Göttingen: Göttingen, Germany, 1997.